Mechanical Modelling of Cavity Wall Metal Ties

O. Arslan
Department Materials, Mechanics, Management & Design, TU Delft, Delft, The Netherlands
Research Centre NoorderRuimte, Groningen, The Netherlands

F. Messali & J. G. Rots
Department Materials, Mechanics, Management & Design, TU Delft, Delft, The Netherlands

E. Smyrou & I. E. Bal
Research Centre NoorderRuimte, Hanze University of Applied Sciences, Groningen, The Netherlands

ABSTRACT: The seismic assessment of unreinforced masonry (URM) buildings with cavity walls is of high relevance in regions such as in Central and Northern Europe, Australia, New Zealand and China because of the characteristics of the masonry building stock. A cavity wall consists of two separate parallel walls usually connected by metal ties. Cavity walls are particularly vulnerable to earthquakes, as the out-of-plane capacity of each individual leaf is significantly smaller than the one of an equivalent solid wall. This paper presents the results of an experimental campaign conducted by the authors on metal wall tie connections and proposes a mechanical model to predict the cyclic behaviour of these connections. The model has been calibrated by using the experimental results in terms of observed failure modes and force-displacement responses. Results are also presented in statistical format.

1 INTRODUCTION

Cavity walls are often used in unreinforced masonry (URM) buildings in many countries, such as in Central and Northern Europe, Australia, New Zealand and China. Double-leaf cavity walls constitute a large portion of the building inventory in the province of Groningen, a large gas field in the north of the Netherlands, where the number of human-induced earthquakes has recently increased. These buildings are subjected to induced earthquakes up to magnitude of 3.6 until now, with the largest recorded horizontal PGA of 0.11g. A cavity wall consists of two separate parallel walls (called leaves), with an inner load-bearing leaf and an outer veneer, that has mostly aesthetic and insulating functions (Fig 1). The inner and outer leaves are interconnected by means of metal ties, as described in NEN-EN 845-1(NEN 2016).

The out-of-plane failure is a common mechanism during an earthquake for this typology of walls, which often stems from poor wall-to-wall, wall-to-floor or wall-to-roof connections, which are unable to provide sufficient restraint and boundary conditions, as well as from the slender geometry of the two parallel leaves.

Lintz & Toubia (2013) proposed a simplified analytical method to determine the amount of load transferred through the ties to the brick veneer and found that placing vertical reinforcement in the outer leaves could allow for an increase of the design strength.

An earlier study by Kobesen (Kobesen et al. 2014) defines the wall tie connection strength based on the pulling out of bars from concrete (Bruggeling et al. 1986, Cement en Beton 2011). In the model of Bruggeling (1986), the reinforcement embedded in concrete and subjected to tension is assumed to have the same strains of concrete. Though it uses slightly different stress and strain profile, Braam and Lagendijk (2011) also provides a similar approach. Kobesen (2014) used the same assumption for metal tie embedded in mortar.

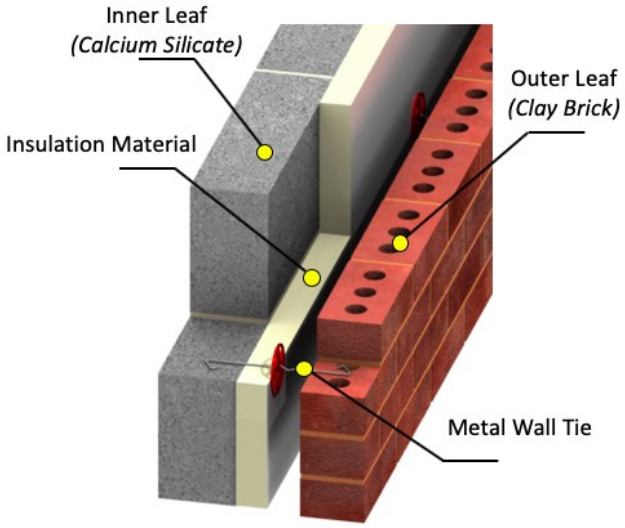

Figure 1. Cavity wall

An experimental campaign was performed at the Delft University of Technology (TU Delft) in 2019 (Arslan et al. 2020) to provide a complete characterization of the axial behaviour of metal connections in cavity walls by means of a dataset of 202 couplets. This work discusses the results presented by

Arslan et al. (2020) from a statistical point of view with the aim to provide recommendations for design standards and guidelines. Both the mean and the characteristic values of the peak force and the displacement at peak force are computed for each group of tests. In addition, a mechanical model is proposed and calibrated against the load-displacement curves obtained for each group of connections.

2 EXPERIMENTAL CAMPAIGN

An experimental campaign on cavity wall ties was carried out at TU Delft to study the axial behaviour of these type of connections in terms of axial strength, force-displacement curve and dissipated energy (Arslan et al, 2020). A large number of variations was considered in the research in order to provide a complete characterization of the connections: two embedment lengths, four pre-compression levels, two different tie geometries, and five different testing protocols, including monotonic and cyclic loading.

Each specimen (couplet) consisted of two bricks and a mortar joint where a metal wall tie was embedded. The couplet was designed to be representative of a portion of as-built URM cavity walls. L-shaped ties with a diameter of 3.6 mm and a total length of 200 mm were placed inside the mortar bed-joint, as happens in real applications. In practice, the zigzag-end is embedded in the CB masonry, while the L hook-end is embedded in the inner CS walls. 202 couplets were tested in total, consisting of four different typologies: CS70, CB50, CS50 and CS70-15D (Fig. 2). A couplet of type CS70 and the test setup is shown in Figure 3.

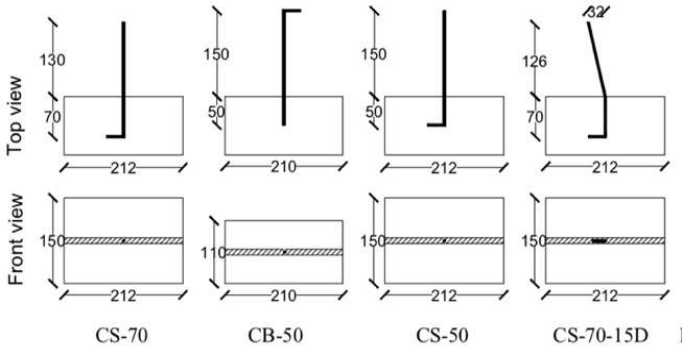

Figure 2. Geometry of tie specimens

In Arslan et al. (2020), the findings of the experimental campaign are reported in terms of failure mechanism, average force-displacement curve, peak force, and displacement at the peak force and at failure, identified as the point of reduction by 20% of the peak force as commonly assumed [Fardis (2009) and Zhang et al. (2015)]. The four different failure modes that were obtained in the experimental campaign are shown in Figure 4. The large majority of the couplets loaded in compression exhibited buckling failure, while in tension the sliding failure prevailed.

A series of companion tests were performed to determine the mechanical properties of the materials used in the experimental campaign, such as the flexural and compressive strength of the mortar, the tensile and compressive capacity of the tie, and the bond strength between masonry units and mortar.

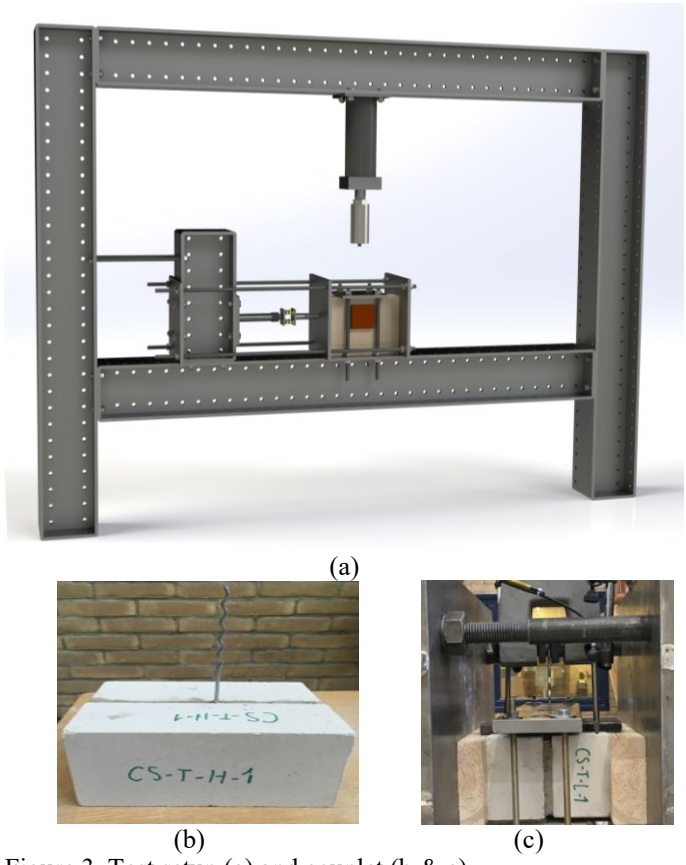

(a) (b) (c)

Figure 3. Test setup (a) and couplet (b & c)

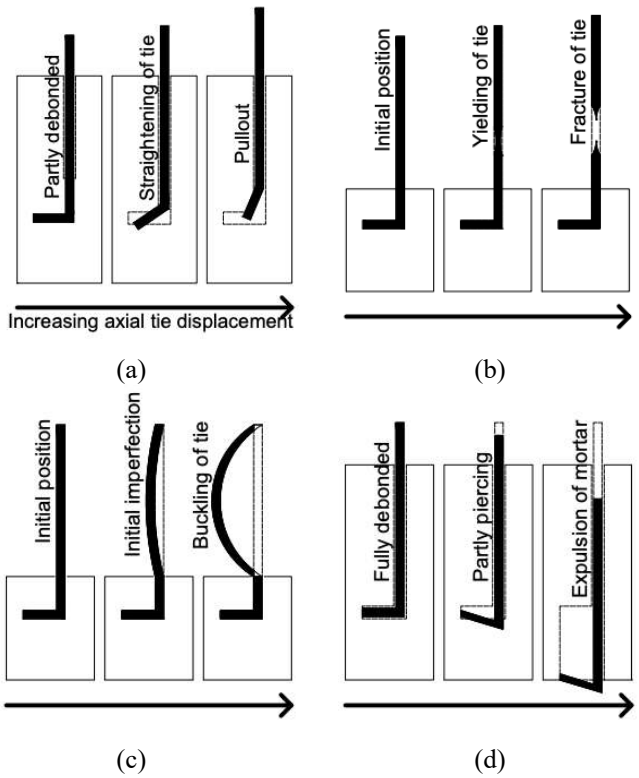

(a) (b) (c) (d)

Figure 4. Failure mode sequence: Type A (a), Type B (b), Type C (c) and Type D (d)

3 STATISTICAL INTERPRETATION OF THE RESULTS

A statistical analysis of the experimental results is performed to compute the median and characteristic values of the peak load and of the displacement at peak load to provide recommendations for guidelines and standards. Besides that, an upper and lower bound for the capacity of the cavity wall tie connection is defined based on the 5th and 95th fractile. The statistical values for each typology (CS70, CB50, CS50 and CS70-15D) are computed according to the procedure proposed in Eurocode 0 (CEN 2005), for both tensile and compression loads, and for monotonic and cyclic loading. When the statistical distribution of a property is not known *a* priori, the characteristic value X_k can be computed as follows:

$$X_k = exp[m_x - (k_n \times s_y)] \quad (1)$$

where m_x is the mean value of a test series, s_y is the standard deviation and k_n is the factor that can be taken from table D1 in Eurocode 0 (CEN 2005). Table 1 summarizes the obtained experimental results and the characteristic values for each typology.

Table 1. Summary of the obtained median results and characteristic values for each typology.

Specimen Type	Loading Protocol	Median Results				Characteristic Values			
		Tensile		Comp		Tensile		Comp	
		Force (kN)	Disp (mm)	Force (kN)	Disp (mm)	Force (kN)	Disp (mm)	Force (kN)	Disp (mm)
CS70	Mono	2.35	10.63	1.77	3.14	1.99	7.80	1.42	2.30
	Cyclic	1.88	6.88	1.73	2.78	1.31	2.86	1.40	1.85
CB50	Mono	3.54	7.02	1.83	2.13	2.70	2.87	1.50	1.72
	Cyclic	3.59	7.64	1.60	0.39	2.87	4.08	1.49	0.13
CS50	Mono	1.87	8.25	1.80	2.52	1.44	6.47	1.16	2.12
	Cyclic	1.62	4.69	1.90	3.41	1.41	3.07	1.46	1.49
CS70-15D	Mono	2.51	13.07	1.35	4.48	2.25	10.61	1.23	2.97
	Cyclic	2.07	9.67	1.44	3.97	1.68	9.19	1.26	2.72

Note: Disp=Displacement; Comp=Compressive; Mono=Monotonic

To have a better understanding of the results, equivalent lognormal distributions are computed for the tensile/compressive strength of each group of connections. A lognormal distribution is selected due to the right skewed nature of the experimental data. The fitting of the original data is conducted by using the method of moments. The obtained distribution is plotted in Figure 5 in terms of cumulative distribution function (CDF) and probability density function (PDF) for the cyclic tests of each examined typology (CS70, CB50, CS70-15D and CB50). The plots show also that the original results exhibit the good correspondence with the lognormal distributions. The CDF curves report the 5th, 50th and 95th fractile values of the dataset distribution.

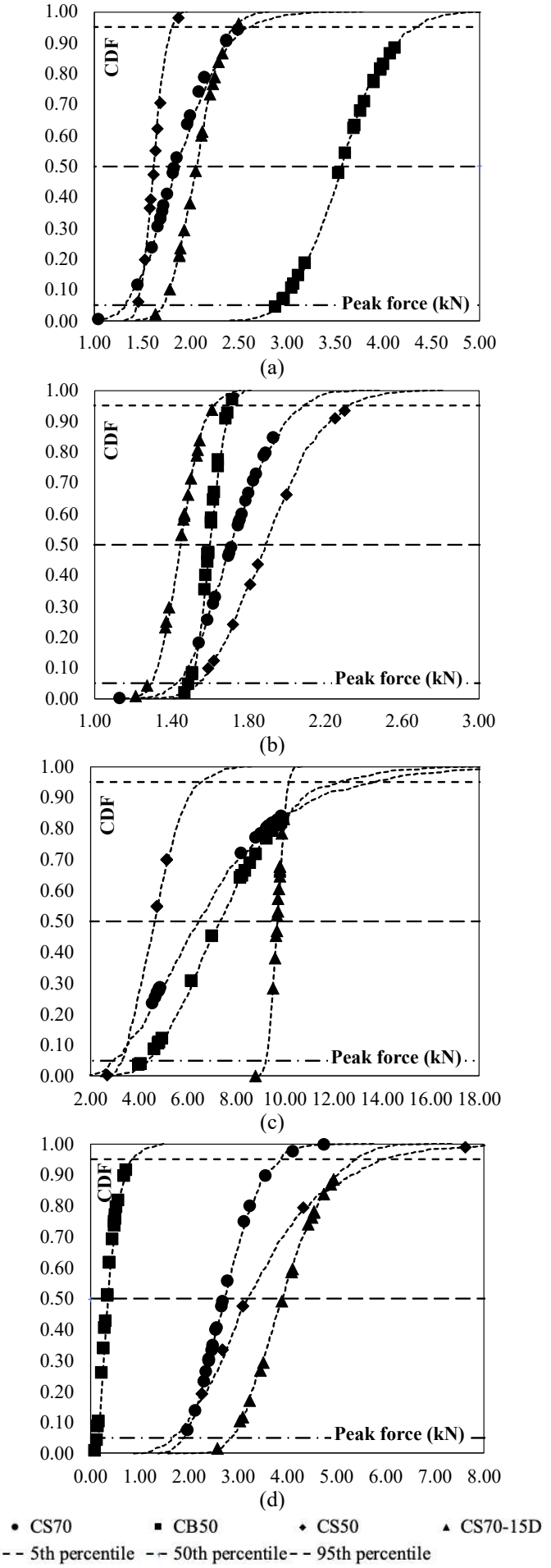

Figure 5. Cumulative functions for the tested typologies: Peak force for Tension (a) and Compression (b), Corresponding displacement for Tension (c) and Compression (d). All the curves are defined for the cyclic tests.

It was observed that the mean value of the peak force from CB50 is higher than in the case of CS70, CS50 and CS70-15D for tensile loading (Fig. 5a), whereas the mean values of the displacement at peak force are all close to each other (Fig. 5b). On the contrary, for compressive loading, all the typologies have similar cumulative curves for both the peak force (Fig. 5c) and the displacement at peak (Fig. 5d).

The PDF of the moments on the experimental results of CS leaf and CB leaf are plotted in the same graph, in order to highlight by which of type of embedment in the two leaves is the overall connection capacity governed (Fig. 6). The PDF curves report also the 5th fractile value of the dataset distribution as well as the characteristic value computed according to Eq. 1. The two results shown in Figure 6 refer to the ideal connections (Fig. 6a) and to imperfect applications in practice, with a bent tie (Fig. 6b). The results for the two cases are very similar. It can be concluded that the behaviour of the wall-tie connection is governed by the tie embedment in the CS leaf. The failure mechanism will occur first in CS masonry, followed by CB masonry. The probability of having the failure in CB masonry before CS masonry is 4.5% for the ideal case (CS70 and CB50), and only 2.4% for the case with bent ties (CS70-15D and CB50).

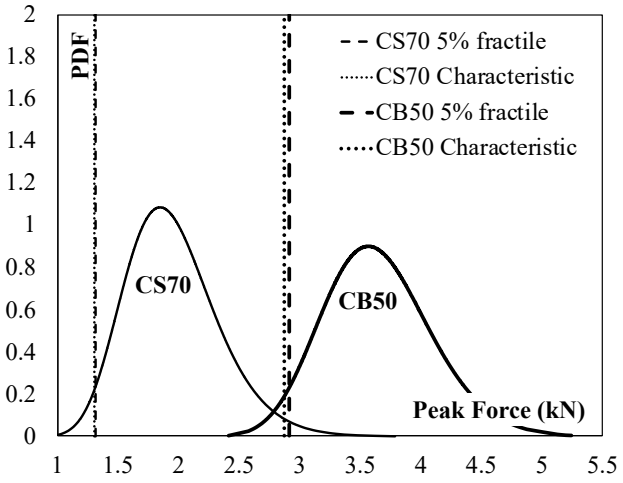

Figure 6 Probability functions for the tested typologies: CS70 and CB50 (a) and CS70-15D and CB50 (b)

4 MECHANICAL MODEL

A mechanical model is developed in order to determine the load and the corresponding displacement. The mechanical model must account for CS and CB units in terms of the force-displacement behaviour and the failure mechanism, as explained above. The test results show that sliding failure of ties (Failure mode A) along the tie-mortar interface was the dominant failure mode in tension. While, the main failure mechanism in compression was buckling of the tie (Failure mode C).

Considering all the failure mechanisms and the experimental results, a simplified envelope curve is proposed for each tested typology to fit the results observed from the experimental campaign. The proposed curve has been produced as simplified approximation after averaging data from the results of the experiment so that the elastic, hardening phase and ultimate phase are defined. The force-displacement curve is idealized into trilinear branches in tension whose input parameters are the yielding strength (F_{Te}), yielding displacement (Δ_{Te}), peak strength (F_T), displacement at the peak (Δ_T), ultimate strength (F_{Tu}) and ultimate displacement (Δ_{Tu}). In compression it is approximated by bilinear branches where the input parameters are the peak strength (F_C), displacement at the peak (Δ_C), ultimate strength (F_{Cu}) and corresponding displacement (Δ_{Cu}), as shown in Figure 5. The proposed curve is valid for CS and CB for all failure modes. However, the calibration of these parameters for the envelope curve are different each of the two materials.

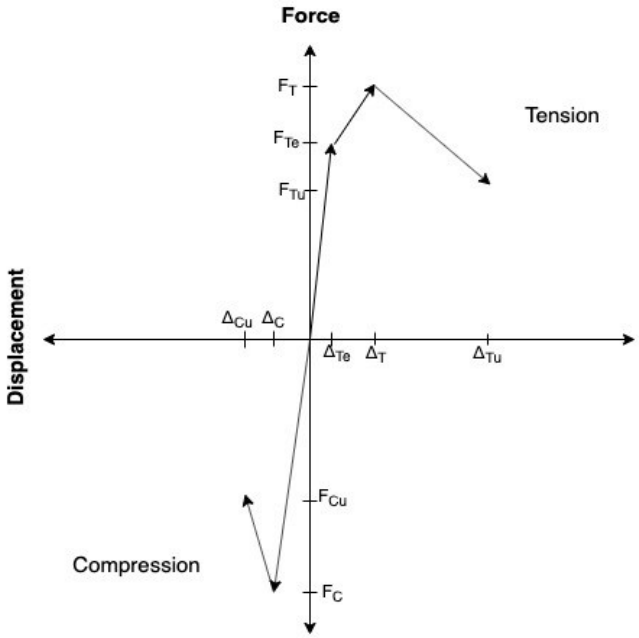

Figure 7. Simplified envelope curve

4.1 *Tensile Strength of the Connection*

The initial stage in tension represents the linear elastic behaviour which is governed by bonding between the tie and mortar. F_{Te} can be computed by using the

bond strength equation, adapted from CEB-FIP (1993) as shown below in Equation 2.

$$F_{Te} = T_{b,max} \times \pi \times \phi \times L_S \quad (2)$$

$$T_{b.max} = a \times \sqrt{f_c} \quad (3)$$

where $T_{b,max}$ is the maximum bond strength, ϕ is the diameter of the tie, L_s is the embedded length of the tie, fc is the compressive strength of the mortar and α is the modification factor for CS and CB, shown in Table 2. Equation 2 is valid for all typologies. The bond-slip model assumes a different modification factor according to the shape of the bar, i.e. plain (CEB-FIP (1993)) or deformed bar (Verderame et al. (2009)), for the interaction mechanism between tie and mortar. CS couplets can be associated to the frictional coefficient between tie and mortar that takes a low value as it represents plain bar condition. In the case of CB, a conservative value has been chosen for the modification factor since the shape of tie where embedded in mortar is zigzag representing thus deformed bar condition.

Table 2. a values taken from CEP-FIP (1993)

	CS	***Clay***
a	0.3	1.5

The peak force in tension (F_T) for CS50 and CS70 can be computed as the summation of the yield strength (F_{Te}) and the hardening force which is the force for straightening of the hooked part computed by the 2nd term in Equation 4. Note that L_H is the hooked length of the tie and σ_S is the tensile strength of the tie.

$$F_T = F_{Te} + \frac{4}{L_H} \times \left(\frac{f_c \times \phi \times {L_H}^2}{2} + \frac{\sigma y \times \pi \times \phi^3}{32}\right) \quad (4)$$

A term accounting for imperfect application in practice is added to Equation 4 yielding in the computation of the peak force for CS70-15D. (Eq. 5). The extra term is the deflection due to bending.

$$F_T = F_{Te} + \frac{4}{L_H} \times \left(\frac{f_c \times \phi \times {L_H}^2}{2} + \frac{\sigma y \times \pi \times \phi^3}{32}\right) + \frac{24 \times E \times I \times \phi}{{L_C}^2} \quad (5)$$

where E is the elastic modulus of the tie, I is the second moment of area of a circle and Lc is the cavity length between two leaves. Regarding CB50, the peak force can be computed using Equation 6, as given below:

$$F_T = F_{Te} + f_c \times \phi \times L_S \quad (6)$$

The peak strength in tension for CB consists of two terms. The first term, adopted from CEB-FIP (1993), stands for the bond-slip and the last term accounts for the zigzag portion of the tie which crushes the surrounding mortar. The ultimate force in tension (F_{Tu}), identified as the point of reduction by 20% of the peak force, can be computed using Equation 7:

$$F_{Tu} = F_T \times 0.8 \quad (7)$$

The experimental results for the displacement at peak force for all typologies exhibit a striking variability which makes it difficult to capture by simple mechanical model. For that reason, a fully empirical approach is proposed to fit to the displacement values of the experimental force-displacement curves in tension and compression.

The displacement at elastic force, Δ_{Te}, is equal to 1 mm adapted from CEB-FIP (1993) for all typologies.

The displacement at peak force, Δ_T, is estimated as follows:

$$\Delta_T = \frac{L_H}{4} + 1 \quad (8)$$

Equation 8 is valid for CS70, CS70-15D and CS50 walls. The displacement at peak force for CB walls, Δ_T, can be computed as follows:

$$\Delta_T = \frac{L_S}{10} + 1 \quad (9)$$

The ultimate displacement in tension (Δ_{Tu}), identified as the corresponding point of reduction by 20% of the peak force on the proposed curve, can be computed using Equation 10. The ultimate displacement formula was derived by using linear equation between the peak force and zero force. Equation 10 is valid for all typologies.

$$\Delta_{Tu} = 0.8 * \Delta_T + 3 \quad (10)$$

4.2 *Compressive Strength of the Connection*

The typical failure mode in compression was by buckling of the tie. The compression strength, F_C, is estimated in terms of strength at Euler's critical load as follows:

$$F_C = \frac{\pi^2 \times E \times I}{K^2 \times {L_C}^2} \quad (11)$$

where K is the column effective length factor. Except for the bent ties, the compression strength can be computed using Equation 11, while regarding the bent ties (CS70-15D), F_C is determined as follows:

$$F_C = \frac{\pi^2 \times E \times I}{K^2 \times {L_C}^2} - \frac{6 \times E \times I \times \phi}{{L_C}^2} \quad (12)$$

The reason that CS70-15D is computed by Equation 12 is due to the geometry of the tie which is bent. K is chosen 0.5 for all typologies due to boundary conditions of the connections (rotation and translation fixed). The ultimate force in compression (F_{Cu}), identified as the point of reduction by 20% of the peak force, can be computed using Equation 13:

$$F_{Cu} = F_C \times 0.8 \quad (13)$$

The displacement at peak force, Δ_C, is equal to 3 mm for CS walls, while it is equal to 1 mm for CB walls adopted from the experimental results. The ultimate displacement in tension (Δ_{Cu}), identified as the corresponding point of reduction by 20% of the peak force on the proposed curve, can be computed using Equation 14, as explained above by using a linear relation.

$$\Delta_{Cu} = 0.8 * \Delta_C + 2 \quad (14)$$

results

A mechanical model is presented based on the experiments conducted. The properties derived from the tests used in the mechanical model are summarized in Table 3.

Table 3. Summary of cavity wall tie connection properties

Material Characteristic	Symbol	Typology			
		CS70	CB50	CS70-15D	CS50
Diameter of the tie (mm)	ϕ	3.6	3.6	3.6	3.6
Embedment length of the tie (mm)	L_S	70	50	70	50
Compressive strength of the mortar (MPA)	fc	5.65	6.47	5.65	5.65
Hooked length of the tie (mm)	L_H	25	-	25	25
Elastic modulus of the tie (MPA)	E	32920	32920	32920	32920
Second moment of area of the tie (mm^4)	I	8.3	8.3	8.3	8.3
Cavity length (mm)	L_C	80	80	80	80
Effective column factor	K	0.5	0.5	0.5	0.5

The estimated values of the mechanical model are compared to the experimental results by grouping them per type of connection and loading protocol, as shown in Figure 8 and in Table 4.

5 CONCLUSIONS

Double-leaf cavity walls are very common in the province of Groningen, an area in the north of the Netherlands subjected to induced earthquakes. The out of plane response of the double-leaf cavity walls is one of the most prominent failure mechanisms for such buildings. The wall-to-wall metallic ties can provide an efficient retain to the out-of-plane collapse of the single leaves, but their strength has not been widely investigated yet.

In this study, cyclic and monotonic tests on CS and CB units are used for proposing the strength and the displacement capacity of the connections according to a statistical interpretation of experimental.

The capacity of the wall-tie connection is mainly governed by the tie embedment in the CS leaf.

Comparing the experimental results with the characteristic values in terms of the peak load, on average the experiments provide 19% larger peak load for tension, and on average 18% larger peak load for compression.

The proposed mechanical model can adequately predict the force-displacement behaviour obtained from the tests.

The Authors believe that the presented model is adequate for structural engineers to model the non-linear seismic response of such structures.

Table 4. Obtained results by mechanical model (differences with experimental results between brackets)

Specimen Type	Loading Protocol	Mechanical Model			
		Tensile		Comp	
		Force	Disp.	Force	Disp.
CS-70	Mono	2.23 (-5.13%)	8.56 (-19.51%)	1.68 (-5.25%)	3.54 (12.92%)
	Cyclic	1.89 (0.75%)	7.25 (5.37%)	1.68 (-2.86%)	3.00 (7.94%)
CB50	Mono	3.32 (-6.23%)	6.00 (-14.48%)	1.68 (-8.10%)	1.00 (-53.10%)
	Cyclic	3.32 (-7.51%)	6.00 (-21.51%)	1.68 (5.03%)	1.00 (155.64%)
CS-50	Mono	2.03 (8.42%)	8.56 (3.73%)	1.68 (-6.79%)	3.54 (40.39%)
	Cyclic	1.72 (6.07%)	7.25 (54.49%)	1.68 (-11.77%)	3.00 (-12.05%)
CS70-15D	Mono	2.54 (0.93%)	8.56 (-34.54%)	1.42 (4.87%)	3.54 (-20.99%)
	Cyclic	2.15 (3.94%)	7.25 (-25.05%)	1.42 (-1.72%)	3.00 (-24.45%)

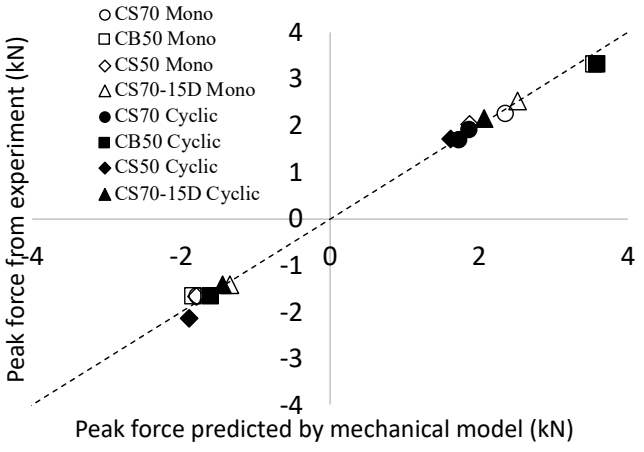

Figure 8. Comparison between experimental results and predicted values by mechanical model for each typology and loading protocol

6 REFERENCE

Arslan O. & Messali F. & Smyrou E. & Bal I. E. & Rots J. G. 2020. Experimental Characterization of Masonry Wall Metal Tie Connections in Double-Leaf Cavity Walls. Man-

uscript submitted for publication.
Braam, C.R. & Lagendijk, ir. P. 2011. Constructieleer Gewapend beton; Cement en beton.
Bruggeling, A.S.J. & De Bruijn, W.A. 1986. Theorie en praktijk van het gewapend beton deel 1, Den Bosch,
CEB-FIP. Model Code 1990. Final draft, Bulletin d'information No. 213/214; 1993.
CEN (2005) EN 1990:2002. Eurocode 0: Basis of structural design. European Committee for Standardisation, Brussels.
Fardis, Michael. (2009). Seismic Design, Assessment and Retrofitting of Concrete Buildings Based on EN-Eurocode 8. 10.1007/978-1-4020-9842-0.
Kobesen M.G. & Vermeltfoort A.T. & Mulders S.G.C. 2014 Wall tie research for existing and new structures; Literature Study. Proceedings of 9th International Masonry Conference, July 7-9, Guimaraes, Portugal.
Lintz, J.M. & Toubia, E.A. 2013. In-Plane Loading of Brick Veneer over Wood Shear Walls. Civil and Environmental Engineering and Engineering Mechanics Faculty Publications. 13.
NEN (2016). NEN-EN 845-1. Specification for ancillary components for masonry - Part 1: Wall ties, tension straps, hangers and brackets. Nederlands Normalisatie-instituut, Delft.
Verderame, G. & de carlo, G. & Ricci, P. & Fabbrocino, G. 2009. Cyclic bond behaviour of plain bars. Part II: Analytical investigation. Construction and Building Materials. 23. 3512-3522. 10.1016/j.conbuildmat.2009.07.001.
Zhang, D. & Waas, A.M. & Yen, Chian-Feng. 2015. Progressive Damage and Failure Response of Hybrid 3D Textile Composites Subjected to Flexural Loading, Part II: Mechanics Based Multiscale Computational Modeling of Progressive Damage and Failure. International Journal of Solids and Structures. 75. 321-335. 10.1016/j.ijsolstr.2015.06.033.